HHS Public Access

Author manuscript

Pain. Author manuscript; available in PMC 2020 July 01.

Published in final edited form as:

Pain. 2019 July ; 160(7): 1594–1605. doi:10.1097/j.pain.0000000000001541.

Somatotopically-specific primary somatosensory connectivity to salience and default mode networks encodes clinical pain

Jieun Kim, Ph.D.[1,2], **Ishtiaq Mawla**[1], **Jian Kong, M.D.**[1,5], **Jeungchan Lee, Ph.D.**[1], **Jessica Gerber**[1], **Ana Ortiz**[1], **Hyungjun Kim, Ph.D.**[2], **Suk-Tak Chan, Ph.D.**[1], **Marco L. Loggia, Ph.D.**[1], **Ajay D. Wasan, M.D., M.Sc.**[4], **Robert R. Edwards, Ph.D.**[3], **Randy L. Gollub, M.D., Ph.D.**[1,5], **Bruce R. Rosen, Ph.D.**[1], and **Vitaly Napadow, Ph.D.**[1,3]

[1]Department of Radiology, Athinoula A. Martinos Center for Biomedical Imaging, Massachusetts General Hospital, Harvard Medical School, Charlestown, MA 02129, USA

[2]Division of Clinical Research, Korea Institute of Oriental Medicine, Daejeon, 34054, Korea

[3]Department of Anesthesiology, Perioperative and Pain Medicine, Brigham and Women's Hospital, Harvard Medical School, Boston, MA 02115, USA

[4]Department of Anesthesiology, Center for Pain Research, University of Pittsburgh, Pittsburgh, PA 15261, USA

[5]Department of Psychiatry, Massachusetts General Hospital, Harvard Medical School, Boston, MA 02215, USA

Introduction

Chronic pain is a highly prevalent and debilitating disorder[21], and neuroimaging research has strongly associated chronic pain severity and suffering with altered brain physiology. Multiple studies have demonstrated altered functional MRI (fMRI) brain connectivity in numerous neuropathic and functional pain disorders[2; 18; 28; 30; 37; 50], including increased cross-network connectivity between several canonical resting-state networks (e.g. salience, sensorimotor, and default mode networks). While multiple studies of chronic pain patients have converged on similar findings, a large sample-size investigation allowing a more reliable evaluation of somatotopic specificity and subgroup analyses with linkage to clinical pain intensity has been lacking.

The salience network is a bilateral network that activates during novel stimulus-driven attention allocation, i.e. when a stimulus stands out from background afference, and is deemed "salient"[43; 45]. The salience network is strongly linked with a ventral attention network and typically encompasses anterior insula/frontal operculum, anterior mid-cingulate cortex, dorsolateral prefrontal cortex and anterior temporoparietal junction (aTPJ)[27; 34; 49]. Spontaneously flaring clinical pain is a highly salient perception, potentially leading to

Corresponding author: Correspondence should be addressed to Vitaly Napadow. #2301, 149 Thirteenth street, Charlestown, MA, 02129. vitaly@mgh.harvard.edu, Phone: +1 617-724-3402; Fax: +1 617-726-7422.

Competing interests

The authors declare no competing interests.

altered salience network connectivity. Additionally, the sensorimotor network, which includes primary somatosensory (S1) cortical representations for different body regions, may receive excessive excitatory input under clinical pain and be important for coding location and severity of this pain. Our prior study demonstrated reduced resting connectivity between different S1 cortical representations for fibromyalgia patients[23]. In fact, several resting-state fMRI studies have suggested that both fibromyalgia and chronic back pain patients exhibit increased cross-network connectivity between salience, sensorimotor, and DMN networks[18; 30; 37]. However, which aspects of chronic pain pathology, such as pain catastrophizing - a psychosocial construct strongly linked with self-referential DMN processing [29], contribute to such cross-network connectivity is unknown.

Furthermore, state properties (i.e. stability) of aberrant cross-network connectivity is important to assess, as alterations in connectivity may be relatively immutable and reflect a fairly stable trait (e.g., linked to living with daily chronic pain) or be a more labile, fluctuating state (e.g., linked to spontaneously flaring clinical pain), and researchers have ascribed both trait and state properties to functional connectivity[7]. With regard to state-like properties of pain, our previous neuroimaging studies in both healthy adults[24] and fibromyalgia patients[23] have shown that experimental nociceptive stimuli increase connectivity between salience network regions (e.g., anterior insula), and contralateral somatotopically-specific S1 cortical representations. Whether clinical pain exerts similar state-like alterations remains to be seen.

Here, we tested the hypothesis that both location and intensity of chronic, clinical pain are encoded by increased connectivity between DMN or salience processing brain regions and somatotopically-specific S1 subregions. We contrasted a large cohort of patients suffering from chronic low back pain (cLBP), one of the most common chronic pain disorders[20], with healthy adults. To experimentally manipulate clinical pain states and test the stability of cross-network connectivity, we adopted a modified version of our model for clinical back pain exacerbation[46]. We then explored the association between altered connectivity and exacerbation-induced changes in clinical pain intensity, further probing how, and under what conditions, the clinical pain state modulates resting-state brain connectivity.

Methods

While most of the data came from a single study (N=174; cLBP=135 (78 Female), HC=39(20F)), in order to further bolster the sample size and power of our analyses, we also included data from cLBP patients and healthy control subjects (N=36; cLBP=17(11F), HC=19(12F)) acquired in a prior 3.0T fMRI study[26], which used similar inclusion and exclusion criteria and the same cLBP phenotype and similar study design. Collectively, resting-state fMRI (rs-fMRI) data from 152 cLBP patients and age- and sex-matched healthy controls (N=58) were available for data analyses. All rs-fMRI data were collected using 3.0T Siemens MRI scanners at the Martinos Center for Biomedical Imaging, Charlestown, MA, USA. This study was conducted in accordance with the Partners Human Research Committee, and informed consent was obtained from all participants.

Participants and back pain exacerbation maneuvers

Inclusion criteria for cLBP patients was as follows: 1) aged 18–60 years, 2) cLBP meeting Quebec Task Force Classification System categories I-II (i.e., patients were unlikely to have significant nerve root involvement, stenosis, or mechanical instability[1; 31]) as confirmed by the study physician and/or review of medical records with the use of previous x-ray reports, 3) duration of low back pain greater than 6 months, 4) severity of low back pain averaging at least 4 on a 0–10 pain intensity scale (0=no pain, 10=most intense pain imaginable) over the past two weeks, and 5) ability to temporarily exacerbate their low back pain using individually-calibrated physical maneuvers. Exclusion criteria for cLBP patients included the following: 1) back pain due to cancer, fracture, or infection, 2) constant radicular pain radiating below the knee, 3) complicated chronic back syndromes (e.g., prior back surgery, ongoing medicolegal issues), 4) active substance abuse disorder in the past two years, 5) history of cardiac, respiratory, or nervous system disease that may impact MRI, 6) use of prescription opioids exceeding 60mg morphine equivalents per day or steroids for pain, (7) acupuncture contraindications (e.g., coagulopathy) or history of acupuncture treatment (due to aims of a separate longitudinal study), and 8) presence of typical contraindications for MRI scanning. Healthy controls aged 18–60 demographically matched to cLBP patients were also enrolled, with exclusion criteria as for cLBP above, in addition to any low back or other acute/chronic pain disorder.

For cLBP patients, a clinical/behavioral session prior to the MRI sessions was used to determine which back-targeted physical maneuvers reliably exacerbated their low back pain. The maneuvers were an individualized, dynamic procedure that controlled the level of movements to briefly increase the intensity of cLBP in an objective, measured, and reproducible manner such that it would remain at this elevated level during the scan session. First, the experimenter and the participant discussed maneuvers that would potentially exacerbate back pain. Participants were informed that they did not have to perform maneuvers if they felt their pain was too severe at baseline pain state. Next, the participant performed a set of typical maneuvers (e.g., toe touches, facet-joint loading twists, sit-ups, back arches, pelvic tilts), and the experimenter recorded parameters (e.g., number of repetitions, extension, angular deviation) of each maneuver, as well as the change in pain severity. If these typical maneuvers were unsuccessful in exacerbating pain, subjects then chose an experience from their daily lives that exacerbated pain (e.g., one study participant experienced intense pain while putting on socks, so the participant performed repeated movements mimicking this action, to exacerbate back pain). This procedure has been adapted following several prior neuroimaging studies using similar techniques to exacerbate clinical low back pain[26; 30; 46].

Subjects were also asked to complete several self-report assessments: low back pain bothersomeness over the past week, current low back pain intensity, Beck Depression Inventory (BDI)[3], Back-Pain Specific Disability (BPSD)[41; 42], the Patient-Reported Outcomes Measurement Information System (PROMIS) scale[11], and Pain Catastrophizing Scale (PCS)[44].

Demographic and clinical data were compared between cLBP and healthy control groups using independent samples *t*-tests, while state variables recorded before versus after low

back pain exacerbation maneuvers in cLBP were contrasted with paired sample *t*-tests (SPSS v.22). Pearson's Chi-Square test was used to assess the difference in sex ratio (male:female) between cLBP and HC. Statistical significance was determined at $p<0.05$.

Resting-state fMRI data acquisition

Brain imaging data were acquired using 3.0 Tesla MRI systems (Siemens, Erlangen, Germany), equipped with a 32-channel head coil (N=169 were acquired using a Siemens Skyra system, while N=41 were acquired using a Siemens Trio system. All rs-fMRI data from the prior study[26] were acquired using a Siemens Trio system. Structural MRI was used for standard space co-registration and applied T1-weighted pulse sequences (Skyra MEMPRAGE: TR/TE1/TE2/TE3/TE4=2530/1.69/3.5/5.36/7.22ms, flip angle=7°, voxel size = 1mm isotropic; Trio MPRAGE: TR/TE = 2200/1.54ms, flip angle=7°, voxel size=1.2mm isotropic). Resting-state fMRI data were collected using T2*-weighed gradient-echo BOLD EPI pulse sequences (Skyra: TR/TE=3000/30ms, flip angle=90°, 44 tilted axial slices, voxel size=2.6×2.6×3.1mm; Trio: TR/TE=3000/30ms, flip angle=85°, 47 tilted axial slices, voxel size=3.0×3.0×3.0mm).

All participants were instructed to keep their eyes open and remain still during the 6-minute resting-state fMRI runs. After a baseline run ($cLBP_{pre}$), cLBP patients were removed from the scanner and performed customized physical maneuvers to temporarily increase their low back pain. Following back pain exacerbation, patients were placed back inside the scanner and a second 6-minute resting-state fMRI run was acquired ($cLBP_{post}$). Our previous study showed that similar physical maneuvers did not induce pain or significantly alter cerebral blood flow in healthy controls[46], hence healthy controls did not perform maneuvers. Subjects verbally rated low back pain intensity on a 0–100 scale (0=no pain, 100=worst pain imaginable) before and after each of the $cLBP_{pre}$ and $cLBP_{post}$ fMRI scans.

Physiological/autonomic data were also collected during Siemens Skyra fMRI scans. Cardiac activity was assessed with electrocardiogram (ECG amplifier ECG100C-MRI, Biopac Systems Inc., Goleta, CA, USA) and finger pulse (ADInstruments, Colorado Springs, CO, USA) data. Respiration data were collected using a custom-built pneumatic MRI-compatible belt system with air pressure transducer (PX138–0.3D5V, Omegadyne, Inc.). In-house scripts were used to filter, process, and annotate the physiological signals. All physiological data were collected at 500Hz. Low-pass filtering was applied to remove MRI gradient and RF noise in both cardiac and respiration data (cutoff frequency: 50Hz). We then applied the MATLAB (R2016b, MathWorks, Natick, MA, USA) software library's peakfinder function to annotate cardiac traces, and algorithm-detected peaks were confirmed by visual inspection.

We excluded fMRI data of 19 cLBP and 4 healthy controls due to excessive head motion with the following criteria: 1) greater than 3 mm translation/rotational motion from initial timepoint or 2) relative frame-wise displacement [38; 39] greater than 2 mm. Additionally, data from six individuals with cLBP were excluded as they were not able to perform physical maneuvers during the MRI session. Resting-state fMRI data from a total of 127 cLBP patients and 54 healthy controls were available for analyses.

Functional S1-seed localization fMRI

At a separate MRI visit, in order to localize the S1 representation for the low back (body region related to pain pathology) and fingers (pain-free body region used as control) for localization and seed connectivity analyses, subjects scanned with the Siemens Skyra also completed evoked pain fMRI scans (TR/TE=3000/30ms, flip angle=90°, 44 tilted axial slices, voxel size=2.6×2.6×3.1mm). To avoid bias in analyses, seed localization was determined in a combined sample of cLBP and healthy controls. Cutaneous electrical stimulation was delivered to the right lower back (over erector spinae muscles) or a control location on the right hand (2^{nd} and 3^{rd} fingers) in separate fMRI scans. Before this fMRI scan, the intensities (electrical current, mA) for painful and non-painful electrical stimuli were individually tailored using the method of limits to evoke 40/100 pain (P40, 0=no pain, 100=worst pain imaginable) and 7/10 moderate but not painful sensation (P0, 0=no sensation, 10=on the verge of pain), respectively. For each 4-minute fMRI scan, these two current intensities were used for 13 P40 and 13 P0 (2-second duration, 25Hz, electrical current: P40=3.5±2.9 mA, P0=1.5±1.4 mA) stimulus blocks, applied in randomized order. The inter-stimulus interval was jittered from 6 to 12 seconds. Preprocessing included RETROICOR[16], motion correction (MCFLIRT-FSL), susceptibility-induced distortion correction (TOPUP-FSL), resampling to 2×2×2mm (3Dresample-AFNI), skull stripping (BET-FSL), and functional-to-functional coregistration (FLIRT-FSL). Following spatial smoothing (FWHM=5mm), and temporal filtering (high-pass frequency=1/42s), general linear modeling (GLM with FEAT-FSL) yielded individual-subject response maps for P40 and P0. A second level fixed-effects analysis calculated the P40-P0 difference map for each individual, and these parameter estimates and their variances were then co-registered to MNI-space (BBREGISTER-Freesurfer) and passed up to a group analysis computing the P40 versus P0 difference map. This P40 - P0 difference map was calculated for each stimulus location (low back and finger) separately, across both cLBP and healthy controls. These combined-group P40 versus P0 difference maps were used for S1 localization of low back and finger representations for nociceptive afference, as well as to define consistent seeds in connectivity analyses (see below).

Resting fMRI data preprocessing

Resting fMRI data were corrected for the physiological artifact (RETROICOR-AFNI), head motion (MCFLIRT-FSL), susceptibility-induced distortion (TOPUP-FSL), and skull-stripped (BET-FSL). Collectively, 68.8% of scans (cLBP: 70.1%, HC: 63.0%) contributed physiological data to correct for cardiorespiratory artifacts in fMRI data using RETROICOR[16]. The proportion of missing physiological data did not differ between cLBP and HC groups (Pearson Chi-square=1.3, p=0.25). Additional sources of artifact were then removed using a GLM. Heart rate and respiratory volume data convolved with cardiorespiratory response functions[12; 13], white matter and cerebrospinal fluid signal regressors identified with the top five principal components using the CompCor algorithm[5; 47] with FAST-FSL tissue segmentation, six translational/rotational motion correction parameters, and a censoring confound matrix of head motion outliers (fsl_motion_outliers-FSL) were included in the GLM as nuisance regressors. Importantly, the global signal was not included in this GLM. The residual signal after regressing out these nuisance signals was then transferred to MNI space (BBREGISTER-Freesurfer), spatially smoothed

(FWHM=6mm), temporally high-pass filtered (high-pass=0.006Hz as in previous publications [19; 23; 37], 3dBandpass-AFNI) and used for connectivity analyses. This resting fMRI data analysis pipeline is displayed in Supplementary Figure 1.

Resting fMRI connectivity: Whole-brain analyses

Dual-regression independent component analysis (ICA) and seed-voxel correlation analyses were used. The dual-regression ICA approach uses data-driven methods to explore salience and default mode network level connectivity. For dual-regression ICA[14; 51], temporally concatenated fMRI data from $cLBP_{pre}$, $cLBP_{post}$, and healthy controls were entered in a group ICA analysis (MELODIC-FSL), without predefined dimensionality constraint. From the group ICs (N=10), the best-fit ICs for the salience and default mode network were selected by calculating spatial correlation with a canonical Beckmann 8 template[4], and visualized to confirm adequate IC definitions (see Supplementary Figure 2 for DMN and SN group IC maps with their respective template).

Seed-voxel correlation analyses were used to evaluate whole brain connectivity maps for apriori-defined regions of interest. Specifically, our seed connectivity analysis was inspired by the results of the dual-regression ICA, which found increased salience network connectivity to $S1_{back}$. For this seed connectivity analysis, we first defined a $S1_{back}$ seed using results from the stimulus-evoked back pain fMRI scan described above. A bilateral $S1_{back}$ mask was created by centering a 6-mm radius sphere on the left (contralateral to the right back stimulation site) $S1_{back}$ peak activation voxel (MNI(x,y,z)=−18,−38,72mm) and mirroring this sphere across the mid-sagittal plane. Averaged fMRI signal from this $S1_{back}$ mask was used as a GLM regressor for each individual.

For both dual-regression ICA and seed-voxel connectivity analyses, resultant connectivity parameter estimate and variance maps for each individual were passed up to group-level difference analyses. Connectivity was then contrast between $cLBP_{pre}$ and $cLBP_{post}$ using a paired sample *t*-test while cLBP and healthy control groups were contrast with an independent samples *t*-test. We used FMRIB's Local Analysis of Mixed Effects (FLAME1+2) to improve mixed-effects variance estimation. We also performed whole-brain linear regression analyses within the cLBP group to assess the association between functional connectivity and subjective measures of clinical pain intensity at the time of the scan. For these analyses, the post- minus pre-maneuver parameter estimate difference map was calculated for each subject, while variance maps were summed for the FLAME1+2 linear regression analysis.

While head motion was addressed by several correction algorithms during data preprocessing, we also compared head motion in cLBP and healthy control groups using different metrics. The number of high motion time-points censored from the fMRI timeseries did not differ significantly between groups ($cLBP_{pre}$=6.6±3.2, HC=5.5±3.3, p=0.15) nor between baseline and post-maneuver scans in cLBP ($cLBP_{post}$=6.2±3.0, p=0.23). All individual rs-fMRI datasets included more than 4 minutes of uncensored data as recommend by Parkes et al.[38] (the maximum number of censored volumes for any dataset were 16 for $cLBP_{pre}$, 15 for $cLBP_{post}$, and 14 for HC at TR=3 sec). We also calculated root-mean-square (RMS) relative head motion estimates. The head motion RMS metric did not

differ between cLBP and healthy groups ($cLBP_{pre}$=0.039±0.022, 0.012~0.119 (mean±SD, range), healthy controls=0.038±0.027, 0.009~0.140; *t*-test p=0.91), but was greater in cLBP patients following maneuvers ($cLBP_{post}$=0.047±0.029, 0.008~0.190) compared to baseline pain state ($cLBP_{post}$ vs $cLBP_{pre}$ paired *t*-test, p<0.001) and was trending when compared to healthy controls ($cLBP_{post}$ vs HC unpaired *t*-test, p=0.053). Thus, analyses were adjusted for this frame-to-frame relative head motion metric (RMS), as well as age and sex, by including these variables as regressors in the GLM. Correction for multiple comparisons was performed using GRF cluster correction (Z>2.3) and corrected p<0.05.

Resting fMRI connectivity: Region of interest analyses

Follow-up region of interest (ROI) analyses were performed to evaluate whether salience network connectivity increased to somatotopically specific brain regions. S1 localizations for the back and finger (similarly determined $S1_{finger}$, MNI(x,y,z)=−42,−20,56mm) were used in follow-up ROI analyses, in addition to another control S1 localization for the face ($S1_{face}$), whose location was drawn from a previous evoked-stimulation fMRI study[35]. We also performed follow-up ROI analyses to evaluate which specific salience network subregions showed altered connectivity with the $S1_{back}$ seed. Candidate salience network subregions included the following right and left nodes: anterior insula (MNI(x,y,z)= ±32,20,−2mm), dorsolateral prefrontal cortex (MNI(x,y,z)=±26,42,32mm), and anterior TPJ (MNI(x,y,z)=±60,−32,32mm), with locations drawn from the $S1_{back}$ connectivity difference map contrasting exacerbated pain ($cLBP_{post}$) versus healthy controls (see Results). Functional connectivity data were extracted from centering a 4-mm radius sphere on the voxel for each ROI and were compared between cLBP and healthy control groups using independent samples *t*-tests, while $cLBP_{pre}$ and $cLBP_{post}$ were contrasted with paired sample *t*-tests at p<0.05 level of significance (SPSS v.22).

Pain catastrophizing subgroup analyses

Our prior cLBP study[30; 37] with a high pain catastrophizing chronic pain cohort (mean PCS was 23, adjust to consistent 0–4 rating scale) linked elevated DMN-insula connectivity with increased clinical pain intensity following physical maneuvers. Our current study enrolled a much larger sample with heterogeneous but, on average, relatively low pain catastrophizing scores (mean PCS was 12.5). Thus, we followed up the above analyses to evaluate DMN connectivity in different pain catastrophizing sub-groups. For cLBP patients for whom PCS scores were collected (N=114, see Table 1), PCS scores ranged from 0 to 38. We divided cLBP patients into equal sample size low-, mid-, and high-PCS tertile subgroups with non-overlapping score ranges (i.e. low PCS: 3.12±1.93, 0~7 (mean±SD, range), mid PCS: 11.53±1.91, 8~15, high PCS: 23.32±6.07, 16~38). In order to test whether PCS status influenced clinical pain-linked DMN connectivity, we evaluated for each PCS subgroup, DMN connectivity changes following physical maneuvers, which were also associated with change in clinical pain following these maneuvers, using identical methods as above.

Results

Demographic and clinical characterization

Compared to healthy controls, cLBP patients demonstrated significantly higher BDI, PROMIS (pain interference) and PCS scores (Table 1). Patients performed a range (and sometimes a combination) of physical maneuvers meant to exacerbate their clinical pain, with toe touches being most common (toe touches: 39.4%, facet joint loading twists: 21.3%, leg raise: 19.7%, back arches: 18.1%, simulated activities of daily life: 8.7%). Physical maneuvers significantly and robustly increased low back pain intensity (pre-maneuvers: 31.9±19.9 (mean±SD), post-maneuvers: 53.7±22.5, $p<0.001$) in most cLBP patients (Figure 1). We did not find significant differences in age ($p=0.92$) or sex (Pearson Chi-square=0.14, $p=0.75$) between cLBP patients and healthy controls (Table 1). While prescription medication use was not pervasive in our sample, the most commons classes of medications in cLBP patients included anti-depressants (11.4%), benzodiazepines (3.5%), and opioids (8.8%) (Supplementary Table 1).

ICA-based Network Connectivity Analysis: Increased salience network connectivity to $S1_{back}$ in cLBP patients

Dual-regression ICA analysis found that, compared to healthy controls, cLBP patients exhibited increased salience network connectivity to the pons, cerebellum, and a S1 cluster overlapping the fMRI-localized responses to nociceptive stimuli applied to the low back ($S1_{back}$, Figure 2A). This increased salience network connectivity to S1 was bilateral following physical maneuvers that robustly increased patients' low back pain (Figure 2B, 2C) compared to healthy controls. Furthermore, after physical maneuvers, cLBP patients demonstrated increased salience network connectivity to other brain regions: paracentral lobule, dorsal posterior cingulate cortex (dPCC), dorsomedial prefrontal cortex (dmPFC), ventromedial prefrontal cortex (vmPFC), pons and cerebellum (Table 2). Specifically, group differences for salience network connectivity to default mode network regions (i.e., dPCC, dmPFC, and vmPFC) revealed reduced anti-correlation in patients with cLBP compared to HC.

We also directly explored salience network connectivity to other, control body area representations in S1 (finger and face). Firstly, a ROI analysis found that even in healthy controls, compared to $S1_{back}$, the $S1_{finger}$ and $S1_{face}$ fMRI signal showed greater anti-correlation with the salience network (e.g., paired *t*-test for right $S1_{back}$ versus right $S1_{finger}$, $p<0.001$; paired *t*-test for right $S1_{back}$ versus right $S1_{face}$, $p=0.006$), while SN connectivity to $S1_{finger}$ versus $S1_{face}$ was not different (paired *t*-test for $S1_{finger}$ versus $S1_{face}$, $p=0.16$). Comparing groups, cLBP patients demonstrated increased salience network connectivity to $S1_{back}$ but not $S1_{finger}$ or $S1_{face}$ (Figure 3). Moreover, while a voxel-wise dual-regression salience network ICA analysis did not find altered connectivity between $cLBP_{post}$ and $cLBP_{pre}$, our more focused S1 ROI analysis did find that following physical maneuvers that exacerbated low back pain, cLBP patients showed increased salience network connectivity to $S1_{back}$ but not to $S1_{finger}$ or $S1_{face}$.

Seed-based Connectivity Analysis: Increased $S1_{back}$ connectivity to specific salience network nodes in cLBP

Following up on results from salience network analyses, the fMRI-localized $S1_{back}$ region was also used in a whole-brain seed connectivity analysis. A whole-brain voxelwise $S1_{back}$ seed connectivity analysis did not find increased $S1_{back}$ connectivity for cLBP patients at baseline compared to healthy controls. However, following low back pain exacerbation by physical maneuvers, cLBP patients demonstrated increased $S1_{back}$ connectivity to several salience network brain regions: anterior insular cortex, dorsolateral prefrontal cortex (dlPFC), and anterior TPJ (Table 3, Figure 4A). Furthermore, $S1_{back}$ connectivity was decreased to non-back representation areas within primary somatosensory/motor cortex (S1/M1). We also found that compared to cLBP patients at baseline, following physical maneuvers these patients demonstrated increased $S1_{back}$ connectivity to anterior TPJ, supplementary motor area (SMA), and decreased connectivity to non-back representation areas within S1/M1 (Figure 4B). A follow-up ROI analysis, found increased $S1_{back}$ connectivity to bilateral anterior insula and dlPFC for cLBP patients at baseline compared to healthy adults (Figure 4C). Following physical maneuvers in cLBP patients, there was increased $S1_{back}$ connectivity to left anterior insula and bilateral anterior TPJ.

Association between $S1_{back}$ and salience network connectivity and clinical pain

To more closely link changes in functional brain connectivity with clinical pain intensity, we performed whole-brain linear regression analyses in cLBP patients. Increased low back pain intensity following individualized, back-targeted maneuvers was correlated with increased $S1_{back}$ connectivity to a cluster centered on left anterior insula ($r=0.36$, Figure 5). While this was the only cluster present in the whole brain analysis, we also evaluated associations for other salience network ROI's that demonstrated increased $S1_{back}$ connectivity post versus pre-maneuvers (from Figure 4C), and found that $S1_{back}$ connectivity to these other salience network regions was not correlated with changes in low back pain intensity (R aIns: $r=0.11$, $p=0.23$; R TPJ: $r=0.09$, $p=0.33$; L TPJ: $r=0.04$, $p=0.63$; R dlPFC: $r=-0.07$, $p=0.41$; L dlPFC: $r=0.00$, $p=1.00$), highlighting the role of left anterior insula in encoding clinical pain intensity.

Increased DMN connectivity to $S1_{back}$ in cLBP patients and response to maneuvers

Compared to healthy controls, cLBP patients at baseline demonstrated increased DMN connectivity to a S1 subregion consistent with the cortical representation of the back (i.e. $S1_{back}$) and leg (Figure 6A, Table 4). Low back pain exacerbation following physical maneuvers decreased DMN connectivity to $S1_{back}$ and increased within-DMN connectivity to medial prefrontal cortex (mPFC) (Figure 6B). Furthermore, change in DMN-S1 connectivity following maneuvers was negatively correlated with change in clinical pain intensity ($R=-0.18$, $p=0.04$), thus greater increase in pain following maneuvers was linked with greater reduction in DMN/S1 connectivity.

Increased DMN connectivity to insula in cLBP patients with high pain catastrophizing

For the whole cLBP patient (N=127) cohort, default mode network connectivity to insula did not differ significantly between cLBP and healthy control groups, nor for cLBP before

versus after pain exacerbation maneuvers. However, when the cLBP cohort was broken up into low-, mid-, and high-PCS cLBP subgroups, the low-PCS subgroup demonstrated elevated DMN connectivity to mPFC following physical maneuvers, which was correlated with increasing pain intensity following maneuvers (r=0.35, p=0.04). DMN connectivity decreased to dorsolateral prefrontal cortex (dlPFC) and cuneus following maneuvers for the mid-PCS subgroup, but these changes were not associated with changes in pain intensity. However, high-PCS cLBP patients demonstrated increased DMN connectivity to right anterior/mid insula (Figure 6C) following maneuvers, and this increase was correlated with post-maneuver change in low back pain intensity (r=0.43, p=0.01). A subsequent ROI analysis found that correlation between change in DMN-a/mIns connectivity and change in low back pain intensity was not found for the low- and mid-PCS subgroups (low-PCS: r=0.22,p=0.21; mid-PCS: r=−0.14,p=0.42). Importantly, the magnitude of post-maneuver increase in clinical pain after physical maneuvers did not differ between these PCS subgroups (ANOVA, F(2)=1.42, p=0.25), and was thus unlikely to influence DMN-a/mIns connectivity results.

Discussion

Improved understanding of how clinical pain states are encoded by brain connectivity aids our understanding of the neurophysiology supporting clinical pain perception, how the neurophysiology of clinical pain differs from evoked experimental pain, and even biomarker development, by introducing candidate quantitative imaging metrics that track clinical pain severity, enhancing our ability to diagnose and treat chronic pain. Evaluation of a large sample (N=127) of cLBP patients found that compared to healthy adults, patients demonstrated increased $S1_{back}$ connectivity to both salience and DMN networks. Pain exacerbation maneuvers increased $S1_{back}$ connectivity to salience network regions, but decreased connectivity to DMN, with greater pain intensity increase linked with greater shifts in these connectivity patterns. Furthermore, only in cLBP patients reporting high pain catastrophizing, DMN connectivity was increased to a cardinal node of the salience network, anterior/middle insula cortex, which was also correlated with the magnitude of increased clinical pain intensity following physical maneuvers. These results aid our understanding of how cross-network connectivity encodes clinical pain intensity and how pain catastrophizing might mediate pain encoding.

Compared to healthy adults, cLBP patients demonstrated augmented salience network connectivity to $S1_{back}$, which was further increased following pain-exacerbation maneuvers. Salience network processing has been associated with re-allocation of attentional resources toward a salient stimulus such as pain[10; 25; 33]. In turn, S1 is a critical component of the nociceptive pathway and is known to receive and process afference in order to encode body location and intensity of nociceptive stimuli[8]. Our previous study found that blood flow to S1 was increased following LBP pain exacerbation[46], and cLBP patients show increased S1 cortical thickness compared to healthy adults[26]. Localizing pain within the body should significantly influence attentional focus, and we thus posit that attentional re-allocation is at least partially mediated by greater information transfer between the salience network and the somatotopically-specific S1 representation of the lower back. Increased salience network/$S1_{back}$ connectivity in $cLBP_{pre}$ (i.e. baseline, resting-state) compared to healthy controls,

might reflect trait-like persistence in altered *intrinsic* connectivity. However, exacerbating clinical pain further amplified salience network/$S1_{back}$ connectivity, suggesting that shifts in information transfer dynamics clearly have state-like properties and likely occur throughout patients' daily experience of flaring and abating pain. In general, altered S1 organization[15; 32] and connectivity[23] have been noted in multiple chronic pain populations, and maladaptive reorganization has been hypothesized to influence behavioral/perceptual deficits such as tactile acuity[9].

Within the salience network, $S1_{back}$ connectivity following cLBP pain exacerbation was specifically increased to anterior insula and linked with increase in back pain intensity. The anterior insula is a key node of the salience network and has been implicated in the salience/affective dimension of pain processing[48], as well as stimulus-driven bottom-up control of attentional resources[45]. Interestingly, our previous study[23] evaluated brain connectivity response to evoked, deep pressure pain applied over the lower leg of chronic pain patients, and found that increased $S1_{leg}$ connectivity to left anterior insula was correlated with self-reported scores of attention to the pain stimulus. Thus, our reported linkage between post-maneuver increases in clinical pain and $S1_{back}$ connectivity to left anterior insula in cLBP patients may reflect increased attentional focus on the location of patients' pain – i.e. low back region.

Additionally, cLBP patients at baseline (pre-maneuvers) showed increased DMN connectivity to $S1_{back}$, suggesting that cLBP patients demonstrate greater intrinsic information transfer between self-referential processing regions and S1 regions coding for the location of nociceptive input. However, pain-exacerbating maneuvers *decreased* this DMN/$S1_{back}$ connectivity (in contrast to the increased salience network/$S1_{back}$ connectivity), and greater DMN/S1 connectivity decrease was associated with greater pain intensity exacerbation. Additionally, cLBP patients, particularly in an exacerbated back pain state, demonstrated *decreased* $S1_{back}$ connectivity to other, non-back, S1 representations compared to healthy adults. Reduced $S1_{back}$ connectivity to non-back S1 areas was also seen when contrasting baseline and exacerbated pain states in cLBP patients. Thus, we propose that when clinical pain is temporarily exacerbated, information transfer from S1 nociception processing regions switches from its "home" network(s), which for cLBP may include both the sensorimotor network and DMN, to salience network nodes such as anterior insula, reflecting a switch toward salience processing of nociceptive afference from the pain-affected body region.

Moreover, we previously found that an evoked, experimental pain stimulus reduces connectivity between the S1 subregion activated by that stimulus and other S1 subregions[23; 24]. We also previously noted reduced resting connectivity between multiple different S1 representations for fibromyalgia patients, who suffer from widespread chronic pain[23]. In healthy adults, Riedle et al. found the converse of this phenomenon: habituation to repeated noxious stimulation (i.e., reduced pain perception) was accompanied by *increased* functional connectivity within the sensorimotor network[40]. Taken together, our current findings support the hypothesis that sustained pain experience in a specific body location leads to a tonic level of elevated somatosensory processing, which then both *increases* resting-state connectivity between the specific S1 subregion coding for ongoing

clinical pain (e.g., low back) and DMN or salience network areas, and *reduces* connectivity between this S1 subregion and other sensorimotor network subregions.

We also found that $cLBP_{post}$ (but not $cLBP_{pre}$) patients demonstrated increased salience network connectivity (or decreased anti-correlation) to DMN regions including mPFC and dPCC, corroborating previous studies demonstrating that chronic pain patients can exhibit increased overlap between salience network regions and DMN[18; 30; 37]. Longitudinal therapy that reduces fibromyalgia pain also reduced DMN-a/mIns connectivity[36], while greater pain reduction following pregabalin pharmacotherapy was associated with greater reduction in PCC/anterior insula connectivity[17]. Our large cohort in this study also allowed for a subgroup analysis to identify factors that might influence how cross-network connectivity encodes pain intensity. While in the whole cLBP cohort, salience network connectivity to DMN regions (or vice versa) was not altered by physical maneuvers or linked with the magnitude of post-maneuver pain increase, a high-PCS cLBP subgroup did demonstrate increased DMN connectivity to an anterior/mid-insula cluster almost identical to that found by our prior studies[30; 37], and greater increase was directly associated with greater increase in post-maneuver clinical pain. Thus, given that on average our cLBP cohort reported a relatively low level of pain catastrophizing (mean PCS score of 12.5, compared to 23 in our prior cLBP study[30], and given the previously described role of the salience network and the known role of the PCC in autobiographical memory and self-referential cognition[6], as well as demonstrated activation of the PCC in response to a cognitive pain catastrophizing task[29], altered connectivity between salience and DMN regions may reflect the dominance of pain self-monitoring cognitions and affect in some chronic pain patients. Thus, a direct linkage between DMN/insula connectivity and pain intensity is more evident when patients also suffer from high negative affect.

Limitations of our study should also be noted. While we attribute findings of altered functional connectivity to clinical pain and saliency/attention, we did not explicitly collect scores of attention regarding low back pain. Future studies should evaluate this link directly using post-scan ratings, as unfortunately online ratings during fMRI would require patients to use potentially overlapping cognitive resources, thereby confounding ratings of pain perception and brain response[22]. Another limitation was that while we found significant changes in brain connectivity using a large cohort of cLBP patients, acquired data were pooled from two different MRI scanners. However, our main findings of increased salience network connectivity to $S1_{back}$ and reciprocal increased $S1_{back}$ seed connectivity to salience network brain regions were also evident in separate single-scanner analyses with subsamples of our dataset (Supplementary Figure 3), suggesting that our findings generalize across different scanners and data samples.

In conclusion, increased information transfer between S1 and salience network regions, particularly anterior insula, likely plays an important role in re-allocating attentional focus and affective coding of somatic nociceptive afference from specific body areas. Additionally, increased information transfer between anterior insula and DMN in cLBP patients, and its association with clinical pain, was strongly influenced by pain catastrophizing.

Supplementary Material

Refer to Web version on PubMed Central for supplementary material.

Acknowledgement

This project was supported by the National Institutes of Health, National Center for Complementary and Integrative Health (P01-AT006663, R01-AT007550, R61-AT009306, P01-AT009965), the National Institute of Arthritis and Musculoskeletal and Skin Diseases (R01-AR064367), and the National Center for Research Resources (P41RR14075, S10RR021110, S10RR023043). Support was also generously provided by the Korea Institute of Oriental Medicine (KSN1621051).

References

[1]. Abenhaim L, Rossignol M, Valat JP, Nordin M, Avouac B, Blotman F, Charlot J, Dreiser RL, Legrand E, Rozenberg S, Vautravers P. The role of activity in the therapeutic management of back pain. Report of the International Paris Task Force on Back Pain. Spine (Phila Pa 1976) 2000;25(4 Suppl):1S–33S. [PubMed: 10707404]

[2]. Baliki MN, Mansour AR, Baria AT, Apkarian AV. Functional reorganization of the default mode network across chronic pain conditions. PLoS One 2014;9(9):e106133. [PubMed: 25180885]

[3]. Beck AT, Ward CH, Mendelson M, Mock J, Erbaugh J. An inventory for measuring depression. Arch Gen Psychiatry 1961;4:561–571. [PubMed: 13688369]

[4]. Beckmann CF, DeLuca M, Devlin JT, Smith SM. Investigations into resting-state connectivity using independent component analysis. Philos Trans R Soc Lond B Biol Sci 2005;360(1457): 1001–1013. [PubMed: 16087444]

[5]. Behzadi Y, Restom K, Liau J, Liu TT. A component based noise correction method (CompCor) for BOLD and perfusion based fMRI. Neuroimage 2007;37(1):90–101. [PubMed: 17560126]

[6]. Buckner RL, Andrews-Hanna JR, Schacter DL. The brain's default network: anatomy, function, and relevance to disease. Ann N Y Acad Sci 2008;1124:1–38. [PubMed: 18400922]

[7]. Buckner RL, Krienen FM, Yeo BT. Opportunities and limitations of intrinsic functional connectivity MRI. Nature neuroscience 2013;16(7):832–837. [PubMed: 23799476]

[8]. Bushnell M, Duncan G, Hofbauer R, Ha B, Chen J-I, Carrier B. Pain perception: is there a role for primary somatosensory cortex? Proceedings of the National Academy of Sciences 1999;96(14): 7705–7709.

[9]. Catley MJ, O'Connell NE, Berryman C, Ayhan FF, Moseley GL. Is tactile acuity altered in people with chronic pain? a systematic review and meta-analysis. J Pain 2014;15(10):985–1000. [PubMed: 24983492]

[10]. Cauda F, D'Agata F, Sacco K, Duca S, Cocito D, Paolasso I, Isoardo G, Geminiani G. Altered resting state attentional networks in diabetic neuropathic pain. Journal of Neurology, Neurosurgery & Psychiatry 2009:jnnp. 2009.188631.

[11]. Cella D, Riley W, Stone A, Rothrock N, Reeve B, Yount S, Amtmann D, Bode R, Buysse D, Choi S, Cook K, Devellis R, DeWalt D, Fries JF, Gershon R, Hahn EA, Lai JS, Pilkonis P, Revicki D, Rose M, Weinfurt K, Hays R, Group PC. The Patient-Reported Outcomes Measurement Information System (PROMIS) developed and tested its first wave of adult self-reported health outcome item banks: 2005–2008. J Clin Epidemiol 2010;63(11):1179–1194. [PubMed: 20685078]

[12]. Chang C, Cunningham JP, Glover GH. Influence of heart rate on the BOLD signal: the cardiac response function. Neuroimage 2009;44(3):857–869. [PubMed: 18951982]

[13]. Chang C, Glover GH. Relationship between respiration, end-tidal CO2, and BOLD signals in resting-state fMRI. Neuroimage 2009;47(4):1381–1393. [PubMed: 19393322]

[14]. Filippini N, MacIntosh BJ, Hough MG, Goodwin GM, Frisoni GB, Smith SM, Matthews PM, Beckmann CF, Mackay CE. Distinct patterns of brain activity in young carriers of the APOE-epsilon4 allele. Proc Natl Acad Sci U S A 2009;106(17):7209–7214. [PubMed: 19357304]

[15]. Flor H, Braun C, Elbert T, Birbaumer N. Extensive reorganization of primary somatosensory cortex in chronic back pain patients. Neurosci Lett 1997;224(1):5–8. [PubMed: 9132689]

[16]. Glover GH, Li TQ, Ress D. Image-based method for retrospective correction of physiological motion effects in fMRI: RETROICOR. Magn Reson Med 2000;44(1):162–167. [PubMed: 10893535]

[17]. Harris RE, Napadow V, Huggins JP, Pauer L, Kim J, Hampson J, Sundgren PC, Foerster B, Petrou M, Schmidt-Wilcke T, Clauw DJ. Pregabalin rectifies aberrant brain chemistry, connectivity, and functional response in chronic pain patients. Anesthesiology 2013;119(6): 1453–1464. [PubMed: 24343290]

[18]. Hemington KS, Wu Q, Kucyi A, Inman RD, Davis KD. Abnormal cross-network functional connectivity in chronic pain and its association with clinical symptoms. Brain Struct Funct 2016;221(8):4203–4219. [PubMed: 26669874]

[19]. Horovitz SG, Fukunaga M, de Zwart JA, van Gelderen P, Fulton SC, Balkin TJ, Duyn JH. Low frequency BOLD fluctuations during resting wakefulness and light sleep: a simultaneous EEG-fMRI study. Hum Brain Mapp 2008;29(6):671–682. [PubMed: 17598166]

[20]. Hoy D, Brooks P, Blyth F, Buchbinder R. The Epidemiology of low back pain. Best Pract Res Clin Rheumatol 2010;24(6):769–781. [PubMed: 21665125]

[21]. Institute of Medicine. Relieving Pain in America: A Blueprint for Transforming Prevention, Care, Education, and Research. Washington (DC), 2011.

[22]. Kenntner-Mabiala R, Andreatta M, Wieser MJ, Mühlberger A, Pauli P. Distinct effects of attention and affect on pain perception and somatosensory evoked potentials. Biological psychology 2008;78(1):114–122. [PubMed: 18328614]

[23]. Kim J, Loggia ML, Cahalan CM, Harris RE, Beissner F, Garcia RG, Kim H, Barbieri R, Wasan AD, Edwards RR, Napadow V. The somatosensory link in fibromyalgia: functional connectivity of the primary somatosensory cortex is altered by sustained pain and is associated with clinical/ autonomic dysfunction. Arthritis & rheumatology (Hoboken, NJ) 2015;67(5):1395–1405.

[24]. Kim J, Loggia ML, Edwards RR, Wasan AD, Gollub RL, Napadow V. Sustained deep-tissue pain alters functional brain connectivity. Pain 2013;154(8):1343–1351. [PubMed: 23718988]

[25]. Kolesar TA, Bilevicius E, Kornelsen J. Salience, central executive, and sensorimotor network functional connectivity alterations in failed back surgery syndrome. Scand J Pain 2017;16:10–14. [PubMed: 28850382]

[26]. Kong J, Spaeth RB, Wey HY, Cheetham A, Cook AH, Jensen K, Tan Y, Liu H, Wang D, Loggia ML, Napadow V, Smoller JW, Wasan AD, Gollub RL. S1 is associated with chronic low back pain: a functional and structural MRI study. Molecular pain 2013;9:43. [PubMed: 23965184]

[27]. Kucyi A, Hodaie M, Davis KD. Lateralization in intrinsic functional connectivity of the temporoparietal junction with salience- and attention-related brain networks. J Neurophysiol 2012;108(12):3382–3392. [PubMed: 23019004]

[28]. Kucyi A, Moayedi M, Weissman-Fogel I, Goldberg MB, Freeman BV, Tenenbaum HC, Davis KD. Enhanced medial prefrontal-default mode network functional connectivity in chronic pain and its association with pain rumination. J Neurosci 2014;34(11):3969–3975. [PubMed: 24623774]

[29]. Lee J, Protsenko E, Lazaridou A, Franceschelli O, Ellingsen DM, Mawla I, Isenburg K, Berry MP, Galenkamp L, Loggia ML, Wasan AD, Edwards RR, Napadow V. Encoding of self-referential pain catastrophizing in posterior cingulate cortex in fibromyalgia. Arthritis & rheumatology (Hoboken, NJ) 2018.

[30]. Loggia ML, Kim J, Gollub RL, Vangel MG, Kirsch I, Kong J, Wasan AD, Napadow V. Default mode network connectivity encodes clinical pain: an arterial spin labeling study. Pain 2013;154(1):24–33. [PubMed: 23111164]

[31]. Loisel P, Vachon B, Lemaire J, Durand MJ, Poitras S, Stock S, Tremblay C. Discriminative and predictive validity assessment of the quebec task force classification. Spine (Phila Pa 1976) 2002;27(8):851–857. [PubMed: 11935108]

[32]. Maeda Y, Kettner N, Holden J, Lee J, Kim J, Cina S, Malatesta C, Gerber J, McManus C, Im J, Libby A, Mezzacappa P, Morse LR, Park K, Audette J, Tommerdahl M, Napadow V. Functional

deficits in carpal tunnel syndrome reflect reorganization of primary somatosensory cortex. Brain 2014;137(Pt 6):1741–1752. [PubMed: 24740988]

[33]. Malinen S, Vartiainen N, Hlushchuk Y, Koskinen M, Ramkumar P, Forss N, Kalso E, Hari R. Aberrant temporal and spatial brain activity during rest in patients with chronic pain. Proceedings of the National Academy of Sciences 2010;107(14):6493–6497.

[34]. Mars RB, Sallet J, Schuffelgen U, Jbabdi S, Toni I, Rushworth MF. Connectivity-based subdivisions of the human right "temporoparietal junction area": evidence for different areas participating in different cortical networks. Cereb Cortex 2012;22(8):1894–1903. [PubMed: 21955921]

[35]. Moulton EA, Pendse G, Morris S, Aiello-Lammens M, Becerra L, Borsook D. Segmentally arranged somatotopy within the face representation of human primary somatosensory cortex. Human brain mapping 2009;30(3):757–765. [PubMed: 18266215]

[36]. Napadow V, Kim J, Clauw DJ, Harris RE. Brief report: decreased intrinsic brain connectivity is associated with reduced clinical pain in fibromyalgia. Arthritis & Rheumatology 2012;64(7): 2398–2403.

[37]. Napadow V, LaCount L, Park K, As-Sanie S, Clauw DJ, Harris RE. Intrinsic brain connectivity in fibromyalgia is associated with chronic pain intensity. Arthritis Rheum 2010;62(8):2545–2555. [PubMed: 20506181]

[38]. Parkes L, Fulcher BD, Yucel M, Fornito A. An evaluation of the efficacy, reliability, and sensitivity of motion correction strategies for resting-state functional MRI. bioRxiv 2017:156380.

[39]. Power JD, Barnes KA, Snyder AZ, Schlaggar BL, Petersen SE. Spurious but systematic correlations in functional connectivity MRI networks arise from subject motion. Neuroimage 2012;59(3):2142–2154. [PubMed: 22019881]

[40]. Riedl V, Valet M, Woller A, Sorg C, Vogel D, Sprenger T, Boecker H, Wohlschlager AM, Tolle TR. Repeated pain induces adaptations of intrinsic brain activity to reflect past and predict future pain. Neuroimage 2011;57(1):206–213. [PubMed: 21514392]

[41]. Roland M, Fairbank J. The Roland-Morris Disability Questionnaire and the Oswestry Disability Questionnaire. Spine (Phila Pa 1976) 2000;25(24):3115–3124. [PubMed: 11124727]

[42]. Roland M, Morris R. A study of the natural history of back pain. Part I: development of a reliable and sensitive measure of disability in low-back pain. Spine (Phila Pa 1976) 1983;8(2):141–144. [PubMed: 6222486]

[43]. Seeley WW, Menon V, Schatzberg AF, Keller J, Glover GH, Kenna H, Reiss AL, Greicius MD. Dissociable intrinsic connectivity networks for salience processing and executive control. J Neurosci 2007;27(9):2349–2356. [PubMed: 17329432]

[44]. Sullivan MJ, Bishop SR, Pivik J. The Pain Catastrophizing Scale: Development and Validation. Psychological Assessment 1995;7:524–532.

[45]. Uddin LQ. Salience processing and insular cortical function and dysfunction. Nat Rev Neurosci 2015;16(1):55–61. [PubMed: 25406711]

[46]. Wasan AD, Loggia ML, Chen LQ, Napadow V, Kong J, Gollub RL. Neural correlates of chronic low back pain measured by arterial spin labeling. Anesthesiology 2011;115(2):364–374. [PubMed: 21720241]

[47]. Whitfield-Gabrieli S, Nieto-Castanon A. Conn: a functional connectivity toolbox for correlated and anticorrelated brain networks. Brain connectivity 2012;2(3):125–141. [PubMed: 22642651]

[48]. Wiech K, Lin C-s, Brodersen KH, Bingel U, Ploner M, Tracey I. Anterior insula integrates information about salience into perceptual decisions about pain. Journal of Neuroscience 2010;30(48):16324–16331. [PubMed: 21123578]

[49]. Yeo BT, Krienen FM, Sepulcre J, Sabuncu MR, Lashkari D, Hollinshead M, Roffman JL, Smoller JW, Zollei L, Polimeni JR, Fischl B, Liu H, Buckner RL. The organization of the human cerebral cortex estimated by intrinsic functional connectivity. J Neurophysiol 2011;106(3):1125–1165. [PubMed: 21653723]

[50]. Yu R, Gollub RL, Spaeth R, Napadow V, Wasan A, Kong J. Disrupted functional connectivity of the periaqueductal gray in chronic low back pain. Neuroimage Clin 2014;6:100–108. [PubMed: 25379421]

[51]. Zuo XN, Kelly C, Adelstein JS, Klein DF, Castellanos FX, Milham MP. Reliable intrinsic connectivity networks: test-retest evaluation using ICA and dual regression approach. Neuroimage 2010;49(3):2163–2177. [PubMed: 19896537]

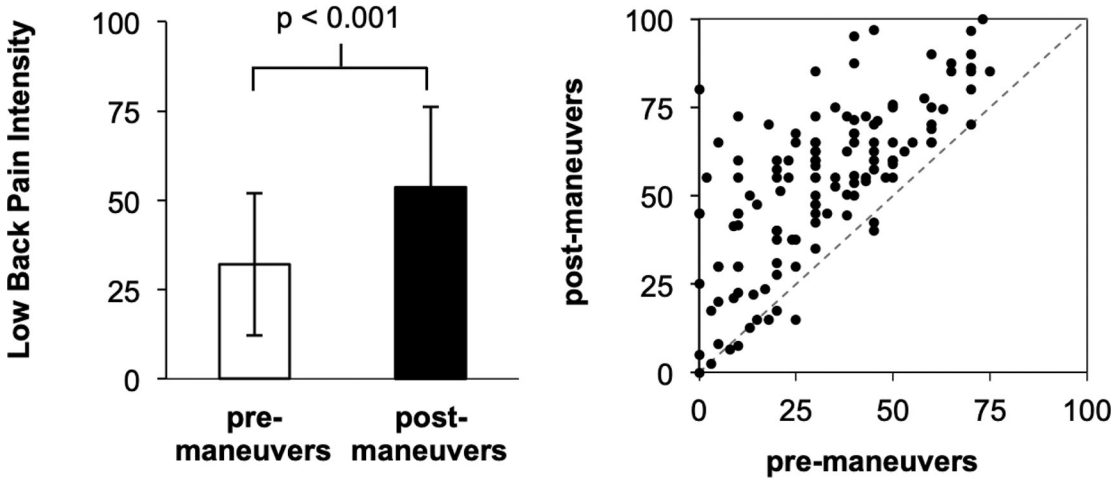

Figure 1.

Low back pain intensity (0–100, numerical rating scale) was significantly increased in cLBP patients following physical maneuvers ($p<0.001$, paired t-test for post-maneuvers versus baseline). Note: error bars represent SD.

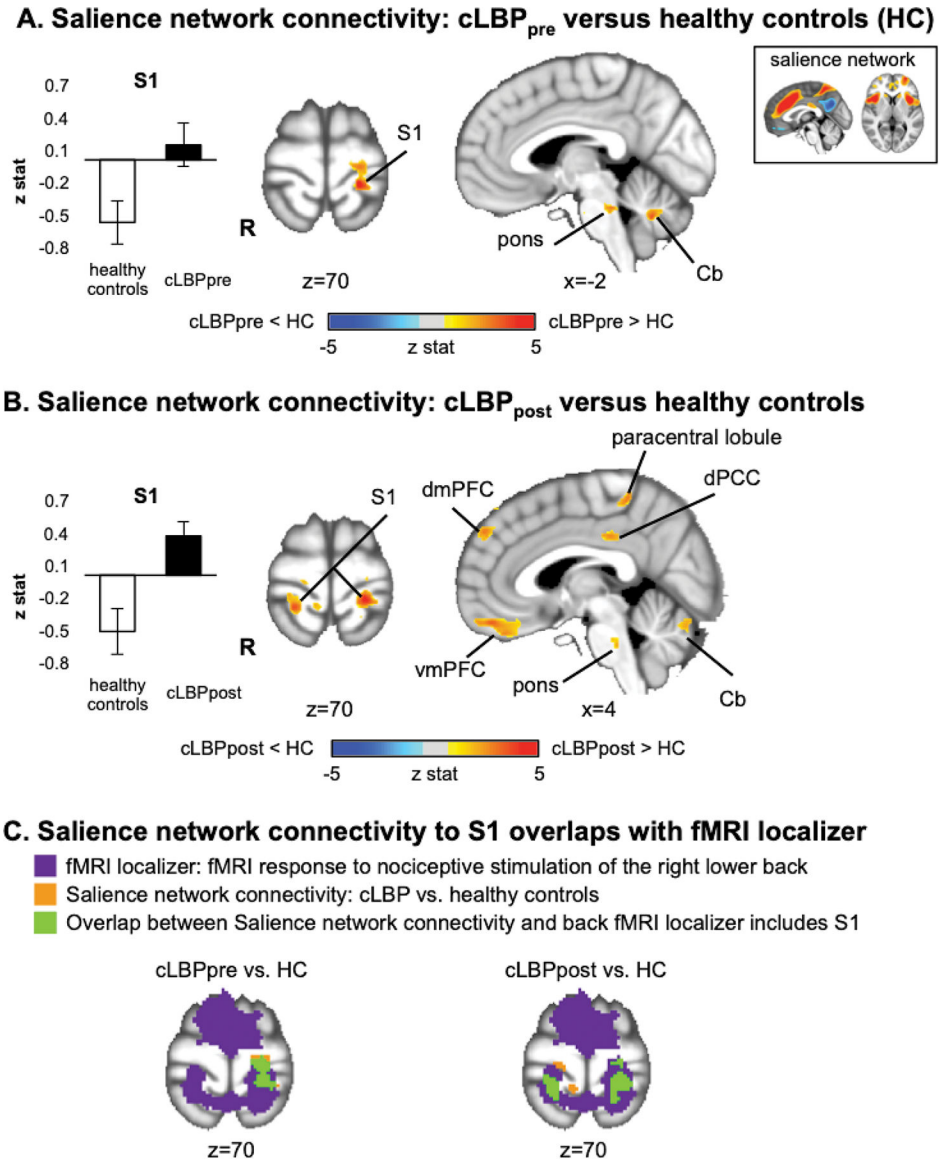

Figure 2.

Dual-regression ICA analysis found that resting salience network connectivity is altered by chronic low back pain. **A.** Compared to healthy controls, cLBP patients exhibited increased salience network connectivity to S1. **B.** Following physical maneuvers that increased patients' clinical low back pain, salience network connectivity was further increased to S1, as well as to several default mode network regions (dPCC, dmPFC, and vmPFC). Note that healthy controls did not perform any maneuvers. **C**. A conjunction analysis found that the S1 subregion noted in A and B partially overlapped (*green*) with the primary sensorimotor cluster found with fMRI-localized response to nociceptive stimulation of the right lower back. Note: S1=primary somatosensory cortex, dPCC=dorsal posterior cingulate cortex, dmPFC=dorsomedial prefrontal cortex, vmPFC=ventromedial prefrontal cortex.

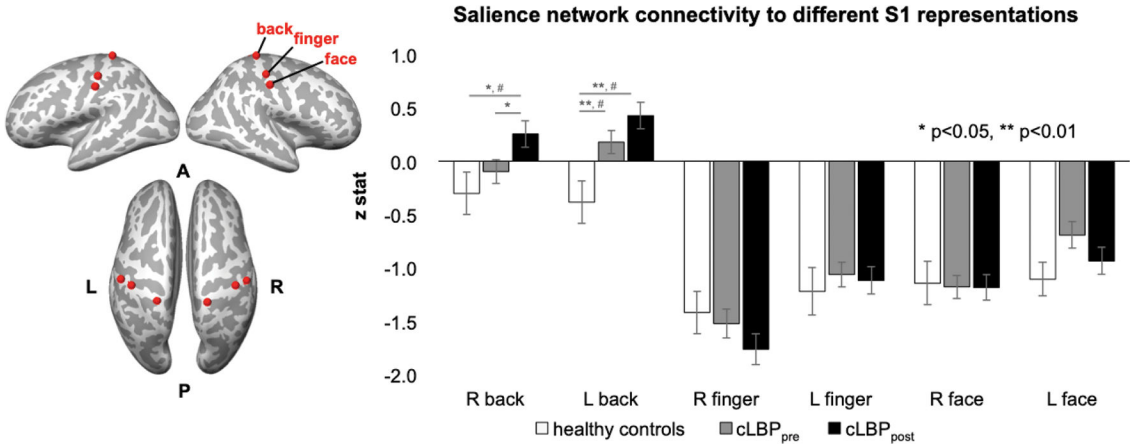

Figure 3.

Salience network connectivity to S1 representations for different body regions. A region of interest (ROI) analysis found that salience network connectivity was increased to $S1_{back}$ but not to $S1_{finger}$ or $S1_{face}$ in cLBP patients compared to healthy controls. Furthermore, connectivity to $S1_{back}$ (but not $S1_{finger}$ or $S1_{face}$) was increased further in cLBP patients following physical maneuvers that exacerbated their low back pain. Note: # = significant with whole brain voxelwise analysis with cluster-size correction for multiple comparisons.

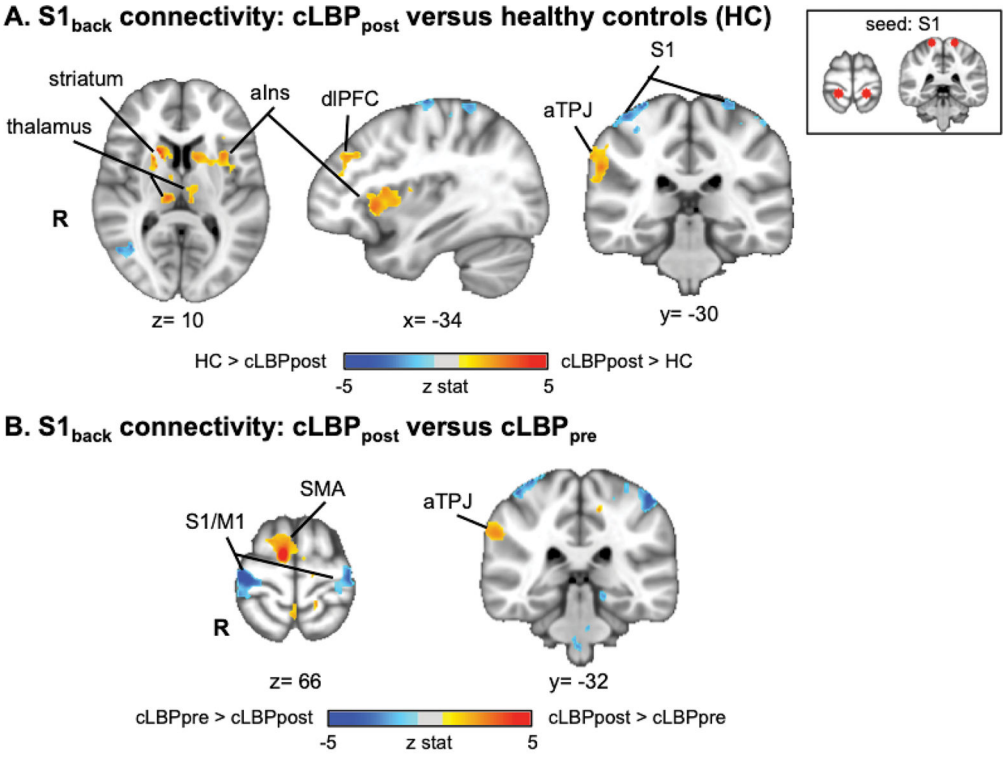

Figure 4.

$S1_{back}$ seed voxel connectivity is altered by exacerbated low back pain in cLBP patients. **A**. Compared to healthy controls, cLBP patients in an exacerbated low back pain state demonstrated increased $S1_{back}$ connectivity to several salience network brain regions: anterior insular cortex (aIns), dorsolateral prefrontal cortex (dlPFC), and anterior temporoparietal junction (aTPJ). Note that healthy controls did not perform any maneuvers. **B**. Compared to cLBP patients at baseline, following physical maneuvers, $S1_{back}$ seed voxel connectivity was increased to anterior temporoparietal junction (aTPJ, a salience network subregion). C. $S1_{back}$ connectivity to specific salience network brain regions was increased in cLBP patients compared to healthy adults. Note: # = significant with whole brain voxelwise analysis with cluster-size correction for multiple comparisons.

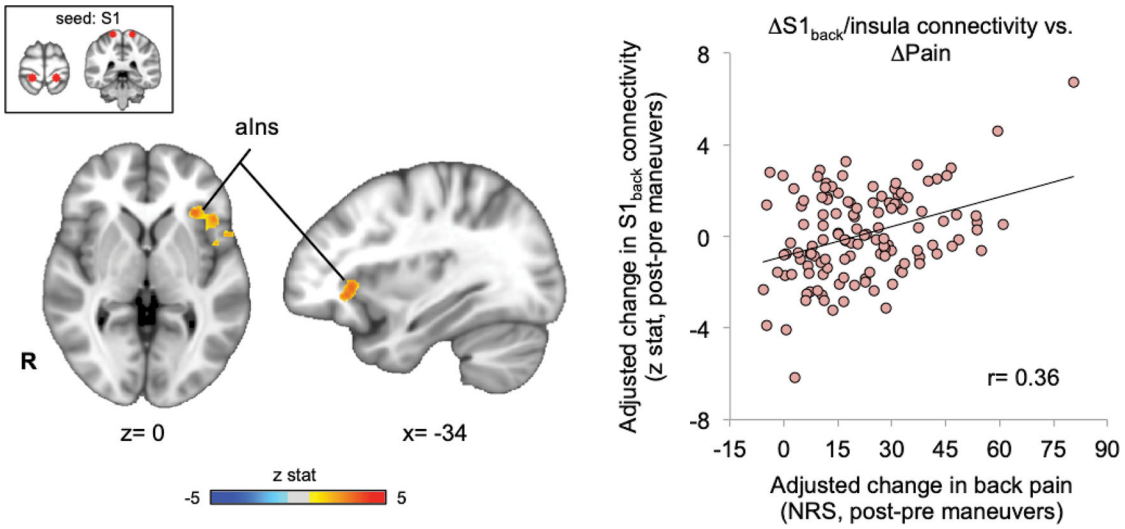

Figure 5.

Maneuvers-induced change in $S1_{back}$ connectivity to anterior insula was associated with change in clinical pain. A whole-brain seed voxel analysis found that physical maneuver induced increase in low back pain was correlated with increased $S1_{back}$ connectivity to left anterior insula cortex. This linear regression analysis was adjusted to control for age and sex, and head motion.

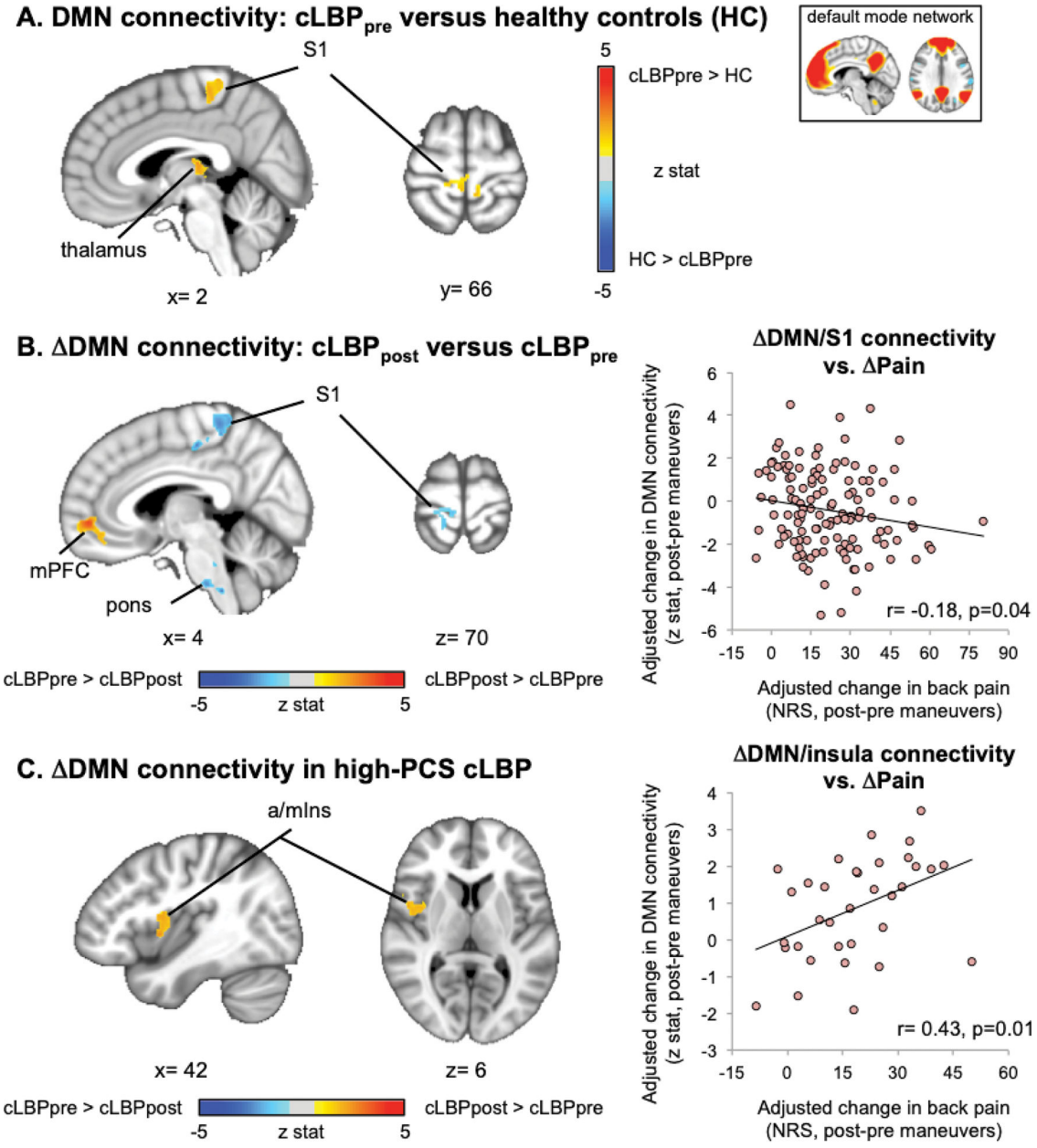

Figure 6.

Default mode network connectivity was altered in cLBP patients and linked with maneuvers-induced change in clinical pain. **A**. Compared to healthy controls, cLBP patients at baseline exhibited increased DMN connectivity to $S1_{back}$. **B.** Following physical maneuvers, DMN connectivity was decreased to $S1_{back}$ and increased to mPFC. Decreased DMN-S1 connectivity was correlated with changes in clinical pain. **C**. In a high-PCS cLBP subgroup increased DMN connectivity to insula after physical maneuvers was associated with post-maneuver increase in low back pain. Linear regression analyses were adjusted to control for age, sex and head motion.

Table 1.

Baseline demographic and clinical data

	cLBP (n=127)	HC (n=54)	p-value
Age (years)	39.3±11.8	39.5±11.2	0.92
Sex (male/female)	55/72	25/29	0.75[1]
Pain duration (years)	7.6±7.0	N/A	-
% using opioids	7.8	0	< 0.001
BDI	6.6±6.9	2.5±4.2	< 0.001
BPSD[2]	8.6±4.5	N/A	-
PROMIS-Physical function[2]	42.3±5.1	56.3±2.8	< 0.001
PROMIS-Pain interference[2]	59.3±5.8	41.6±0.0	< 0.001
PCS[2]	12.5±8.8	4.1±6.0	< 0.001
Back pain bothersomeness[2]	5.1±2.0	N/A	-

BDI Beck Depression Inventory II (0–63 scale), ***BPSD*** Back Pain Specific Disability (0–10 scale), ***PROMIS*** Patient-Reported Outcomes Measurement Information System, ***PCS*** Pain Catastrophizing, Back pain bothersomeness (0–10 scale).

*(1)*Pearson Chi-Square test (2-sided, 0 cells have expected count less than 5)

*(2)*data available for large subset of subjects (cLBP: n=114, HC: n=36)

Table 2.

Salience Network connectivity in healthy controls versus cLBP patients, pre- and post-physical maneuvers, which temporarily exacerbated clinical pain.

	side	size (mm^3)	MNI coordinates			peak z-stat
			X (mm)	Y (mm)	Z (mm)	
$cLBP_{pre}$ versus healthy controls						
S1	L	5,160	−20	−34	70	4.55
cerebellum	R	1,616	14	−58	−36	3.67
	L	13,832	−22	−76	−30	5.34
pons/brainstem	R	4,616	14	−34	−20	3.76
	L	6,880	−10	−32	−20	4.12
$cLBP_{post}$ versus healthy controls						
S1	R	1,160	22	−40	70	4
	L	848	−22	−36	70	4.51
paracentral lobule	L	6,040	−14	−34	56	4.62
vmPFC	R	5,552	8	48	−18	4.02
dmPFC	L	3,288	−4	52	38	4.7
	L	456	−4	42	52	3.08
dPCC	R	576	4	−28	34	3.49
cerebellum	L	21,888	−36	−54	−28	4.5
pons	R	816	6	−26	−30	3.21
$cLBP_{post}$ versus $cLBP_{pre}$						
middle frontal gyrus	R	7,144	54	−62	46	−4.52

S1=primary sensory cortex, vmPFC=ventromedial prefrontal cortex, dmPFC=dorsomedial prefrontal cortex, dPCC=dorsal posterior cingulate cortex

Table 3.

$S1_{back}$ seed connectivity in healthy controls versus cLBP patients, pre- and post-physical maneuvers, which temporarily exacerbated clinical pain.

	side	size (mm^3)	MNI coordinates			peak z-stat
			X (mm)	Y (mm)	Z (mm)	
$cLBP_{pre}$ versus healthy controls						
inferior temporal gyrus	L	4,040	−56	−70	−8	−3.86
precuneus	R	3,488	34	−76	40	−4.09
	L	10,632	−14	−76	48	−4.46
$cLBP_{post}$ versus healthy controls						
anterior insula	L	11,704	−32	20	−2	4.43
anterior TPJ	R	3,736	60	−32	30	3.7
dlPFC	R	3,976	28	40	44	4.09
	L	4,840	−26	42	32	4.09
dmPFC	L	4,544	−2	20	52	3.72
striatum	R	1,696	18	18	4	4.74
	L	1,576	−28	−10	−2	3.25
thalamus	R	776	10	−22	10	3.93
	L	488	−6	−8	−8	3.14
S1	R	3,880	42	−28	64	−3.84
paracentral lobule	L	3,560	−42	−24	66	−3.82
inferior temporal gyrus	R	3,400	42	−62	0	−4.26
$cLBP_{post}$ versus $cLBP_{pre}$						
dlPFC	R	7,000	46	8	40	4.31
anterior TPJ	R	4,776	60	−38	34	3.85
SMA	R	4,008	10	−6	68	5.45
S1	L	1,696	−14	−36	54	3.9
precuneus	R	4,288	12	−76	48	4.53
S1/M1	R	18,744	46	−16	62	−5.4
	L	16,880	−42	−14	60	−4.53
inferior temporal cortex/ parahippocampal gyrus	R	5,680	42	−12	−42	−4.08
superior temporal cortex	L	4,680	−52	16	−18	−3.77

TPJ=temporoparietal junction, dlPFC=dorsolateral prefrontal cortex, dmPFC=dorsomedial prefrontal cortex, S1=primary sensory cortex, SMA=supplementary motor area

Table 4.

Default mode network (DMN) connectivity in healthy controls versus cLBP patients, pre- and post-physical maneuvers, which temporarily exacerbated clinical pain.

	side	size (mm^3)	MNI coordinates			peak z-stat
			X (mm)	Y (mm)	Z (mm)	
$cLBP_{pre}$ versus healthy controls						
S1	L	3,744	−6	−24	54	3.64
thalamus	L	3,184	−18	−38	4	3.49
S1	L	3,032	−62	−20	32	−3.83
$cLBP_{post}$ versus healthy controls						
precuneus	R	7,544	34	−76	34	3.63
$cLBP_{post}$ versus $cLBP_{pre}$						
• All cLBP patients						
mPFC	R	3,672	4	52	−4	4.34
MT+	R	7,888	44	−80	10	4.56
S1/M1	R	5,368	2	−36	66	−3.72
pons	L	3,424	−12	−24	−34	−3.81
• high-PCS cLBP subgroup						
anterior/mid insula	R	2,992	40	4	0	3.34
• mid-PCS cLBP subgroup						
cuneus		9,248	0	76	14	−4.28
dlPFC	R	2,792	46	44	8	−4.09
• low-PCS cLBP subgroup						
mPFC	R	4,880	4	38	−12	4.63
S1/M1	R	4,640	10	−28	72	−4.37

S1=primary sensory cortex, mPFC=medial prefrontal cortex, dlPFC=dorsolateral prefrontal cortex